Metachromasy. IV. The Simultaneous Determination of the Bound Dye Spectra and the Equilibrium Constants between Metachromatic Dyes and Various Polyelectrolytes by the Extended Principal Component Analysis Method

Kiwamu YAMAOKA* and Mineo TAKATSUKI

Faculty of Science, Hiroshima University, Higashisenda-machi, Hiroshima 730

(Received June 3, 1978)

Fourteen sets of visible absorption spectra of two metachromatic dyes, Crystal Violet (CV) and Trypaflavine (TF), were measured in the presence of seven widely different polyelectrolytes—sodium polyphosphate, polyacrylate, and poly(ethylenesulfonate), sodium and potassium poly(*p*-styrenesulfonate)s, and native and denatured calf thymus DNA—in polymer residue-to-dye ratios between 0 : 1 and about 1 : 1. The optical titration curves of these dye-polyanion systems showed either of two changes, sigmoidal or monotonous. The method of principal component analysis was applied to the observed spectra of each dye–polyanion system in order to determine both the equilibrium constant of the binding reaction and the pure spectrum of the bound dye. An empirical parameter α was introduced into the expression for the equilibrium constant in such a way that $K=[\text{complex}]/[\text{free dye}][\text{unoccupied binding site}]^{\alpha}$, by which the sigmoidal titration curves could be reproduced only with $\alpha>1$ and the monotonous ones, with $\alpha\leqq1$. The spectra of bound CV and TF showed metachromasy bands, which depend on the functional group and the conformation of the polyanions, in wavelength regions both shorter and longer than the peak wavelength of the free dyes.

Metachromasy is the well known phenomenon of the spectral change in staining dyes in the presence of polyelectrolyte in aqueous solution. A new absorption band often appears in the wavelength region shorter than the peak wavelength of free dye; it is called the *metachromasy* band (hereafter denoted as the Meta band). Various types of metachromasy, however, have been observed for different combinations of dyes and polyelectrolytes.[1–30] For example, metachromatic changes in Crystal Violet (CV, a triphenylmethane dye)[2] and Trypaflavine (TF, an acridine dye)[3] have been shown to depend on the degree of polymerization of sodium polyphosphate (NaPP) in solution. A remarkable Meta band appears in the CV–NaPP system, whereas no such band is apparent in the TF–NaPP system. Shirai *et al.*[29,30] recently reported that the peak position of the Meta band of Methylene Blue depends on the functional group of polyanions. Since metachromasy is a complicated phenomenon involving a multiple binding between dye and polyanion, it is necessary to know the pure absorption spectrum of the bound dye and the equilibrium scheme between the reaction components for quantitative and systematic studies. Nevertheless, surprisingly few spectra of bound dyes have been unraveled so far,[16,22,31] although the spectra of dimeric dyes have been determined in the absence of polymers.[32–36]

The method of principal component analysis (the PCA method)[37–39] was previously extended and successfully applied to the absorption spectra of various dyes for the simultaneous determinations of not only the number of absorbing components involved in equilibrium mixtures, but also their molar absorption coefficients, and of the equilibrium constant for the acid-base or dimerization reaction.[32] In the PCA method, only the initial concentrations of components and a set of observed absorption spectra are needed as experimental data. It is not necessary to measure the equilibrium concentrations of the various components by experiments such as equilibrium dialysis,[12,16,31] the use of which is limited by the size of permeable molecules of a relatively low molecular weight, the ionic strength of solution, and the dyes extremely adsorbable to the dialysis membrane. The PCA method circumvents these difficulties and should be suited for the determination of an equilibrium scheme for the binding of dye to polyelectrolyte.

In this investigation, the PCA method was applied to fourteen dye–polyelectrolyte combinations in order to obtain information necessary for the quantitative study of metachromasy. As sample dyes, cationic CV and TF were chosen because of their different metachromatic behavior,[1–3] while anionic polyelectrolytes were selected from the point of view of their backbone structure, functional group, and counter-ion. The pure spectrum of the bound dye and the equilibrium constant for the binding reaction were estimated for each dye–polyanion complex system. The results revealed that, in each case, the spectrum of the bound dye has the Meta bands in the wavelength regions shorter and longer than the pronounced peak of the free dye. The peak positions of these bands were found to depend on the functional group and conformation of the polyanions. These are important findings for investigating metachromasy quantitatively in terms of the electronic states of bound dye.[9,40] The optical titration data showed two types of titration curves, sigmoidal and monotonous, depending on the particular combinations of CV or TF with polyanions. An empirical parameter α was introduced into the equilibrium expression for the binding reaction between a dye and a polyanion. By using the parameter α, which may characterize the binding process, the sigmoidal and monotonous optical titration curves could be reproduced successfully.

Experimental

Materials. The dyes, CV and TF, are the same samples as were reported previously.[2,32] The number-average degree of polymerization ($\bar{n}$) of sodium polyphos-

phate (NaPP) is 154, the highest refractionated sample in the previous study.[2] Purified sodium polyacrylate (NaPA, mol wt 7.24×10^5) was described elsewhere.[41] The sodium poly(ethylenesulfonate) (NaPES, $\bar{n}=65$) was a gift of Dr. Masamitsu Shirai of the University of Osaka Prefecture. The potassium poly(*p*-styrenesulfonate) (KPSS, mol wt *ca.* 7.5×10^5) was given by Dr. Koshiro Yoshioka of the University of Tokyo. Both samples were used without further purification. Native calf thymus DNA (nDNA) was purchased from Worthington Biochemical Corp. and was heat-denatured to prepare the denatured sample (dDNA).[31] Sodium poly(*p*-styrenesulfonate) (NaPSS) was prepared by dialyzing the KPSS, which had been dissolved in 3 M aqueous NaCl, against a 1 M NaCl aqueous solution for two days and then against distilled water for four days. All the polyanion samples except DNA were dried *in vacuo* at 56 °C for 6 h and used to prepare the stock solutions (*ca.* 10^{-2} M). Just prior to the absorption measurements, the stock solutions were diluted with distilled water to the desired concentrations.

Procedures. Two matched pairs of 1.0 and 2.0 cm quartz cells were used for CV and TF respectively. The inner wall of the sample cell was pre-equilibrated with a concentrated dye solution to avoid errors due to the adsorption of the dye. The dye adsorbed on the wall was calibrated against distilled water in a clean reference cell. The sample cell was dried and then filled with a fixed volume (3.5 and 7 ml for 1.0 and 2.0 cm cells respectively) of a dye solution. The concentration of the dye solution was optically determined from the molar absorption coefficient ε (9.20×10^4 at 592 nm for CV, 4.67×10^4 at 452 nm for TF) immediately before the addition of a polyanion solution, since the adsorption of dye to galssware is unavoidable and since the actual concentration of the stock dye solution was inevitably reduced in storage.

The series of the absorption spectra of a dye solution were measured by titrating it with a polyanion solution delivered through a microburet. The volume change of the titrate was made as small as possible so as not to shift the binding equilibrium. The volume correction was made for the observed absrobance A_{obsd} which was read out to the maximum of four digits:

$$A = A_{obsd}\frac{v_i+v_{add}}{v_i},$$

where v_i and v_{add} are the initial volume of the dye solution, and the volume of the polyanion solution added to it, respectively.

Measurements. A Hitachi Model EPS-3T recording spectrophotometer was used. The temperature of the cell holder was kept at 25 °C by circulating water through it. The solutions in the cells were always equilibrated for 5—10 min before measurements.

The Concept of the Extended Principal Component Analysis Method

A detailed description of the PCA method and of its application to the equilibrium systems of dye molecules was given in a previous paper;[32] therefore, the concept of the extended PCA method is described here only briefly. In an equilibrium system which contains p absorbing components out of a total of q components, m different absorption spectra can be measured by varying the compositions between these components. This suggests that some correlation must exist between the m absorption spectra because of the contribution from the p absorbing components. These m absorption spectra can be expressed by a data matrix **D** whose element, $D_{ij}(i=1,\ m$ and $j=1,\ n)$, denotes the absorption coefficient of the ith spectrum at the jth selected wavelength. According to Beer's law, the **D** matrix must be represented by the product of a concentration matrix **C** and an absorption coefficient matrix $\boldsymbol{\varepsilon}$:

$$\mathbf{D} = \mathbf{C}\boldsymbol{\varepsilon} = \begin{pmatrix} C_{11} \cdots C_{1j} \cdots C_{1p} \\ \cdots\cdots\cdots\cdots \\ C_{i1} \cdots C_{ij} \cdots C_{ip} \\ \cdots\cdots\cdots\cdots \\ C_{m1} \cdots C_{mj} \cdots C_{mp} \end{pmatrix} \begin{pmatrix} \varepsilon_{11} \cdots \varepsilon_{1j} \cdots \varepsilon_{1n} \\ \cdots\cdots\cdots\cdots \\ \varepsilon_{i1} \cdots \varepsilon_{ij} \cdots \varepsilon_{in} \\ \cdots\cdots\cdots\cdots \\ \varepsilon_{p1} \cdots \varepsilon_{pj} \cdots \varepsilon_{pn} \end{pmatrix} \tag{1}$$

where C_{ij} is the equilibrium concentration of the jth component in the ith solution, and ε_{ij} is the molar absorption coefficient of the ith component at the jth selected wavelength. The matrices, **C** and $\boldsymbol{\varepsilon}$, however, are not known *a priori* in most cases. Hence, the purpose of the application of the PCA method to chemical equilibria is to determine those unknown quantities simultaneously.

In the PCA method, the second moment matrix **A** is first constructed by the product of the **D** matrix and its transposed matrix. The eigenvectors $\boldsymbol{e}_i(i=1,\ n)$ and the eigenvalues $\Lambda_i(i=1,\ n)$ of the **A** matrix can then be calculated by diagonalization. The eigenvectors are the fundamental components which are common to the m absorption spectra, while the eigenvalues represent the contribution of the corresponding eigenvectors to the m spectra.[32] The relation between A_{jk}, Λ_i, and e_{ik} is given as

$$\sum_{j=1}^{n} A_{jk}e_{ij} = \Lambda_i e_{ik}. \tag{2}$$

The eigenvectors giving rise to extremely large eigenvalues are considered to be the principal components. When the eigenvalues are arranged in the order of magnitude, the following relation must hold for the data matrix **D** composed of p absorbing components:

$$\Lambda_1 \geqq \Lambda_2 \geqq \cdots \geqq \Lambda_p \gg \Lambda_{p+1} \geqq \cdots \geqq \Lambda_n > 0. \tag{3}$$

The **D** matrix can, then, be represented by a linear combination of p eigenvectors:

$$\mathbf{D} = \mathbf{f}\boldsymbol{e}, \tag{4}$$

where the **f** matrix of the (m,p) type is a linear combination coefficient matrix and can be calculated by the least-squares method. The $\boldsymbol{\varepsilon}$ matrix can also be related to the p eigenvectors by means of a transformation matrix **t** of the (p,p) type as follows:[32]

$$\boldsymbol{\varepsilon} = \mathbf{t}\boldsymbol{e}. \tag{5}$$

Therefore, the concentration matrix **C** can be computed as follows:

$$\mathbf{C} = \mathbf{f}\mathbf{t}^{-1}. \tag{6}$$

In order to determine the values of the elements of the **t** matrix, an appropriate equilibrium expression must be assumed for the system containing q components in which the absorbing components are p ($p\leqq q$). In the present work, the following general expression was assumed to describe the binding reaction between a dye and a polyanion:

$$K = \prod_{i=1}^{q} [\mathrm{X}_i]^{\nu_i}, \tag{7}$$

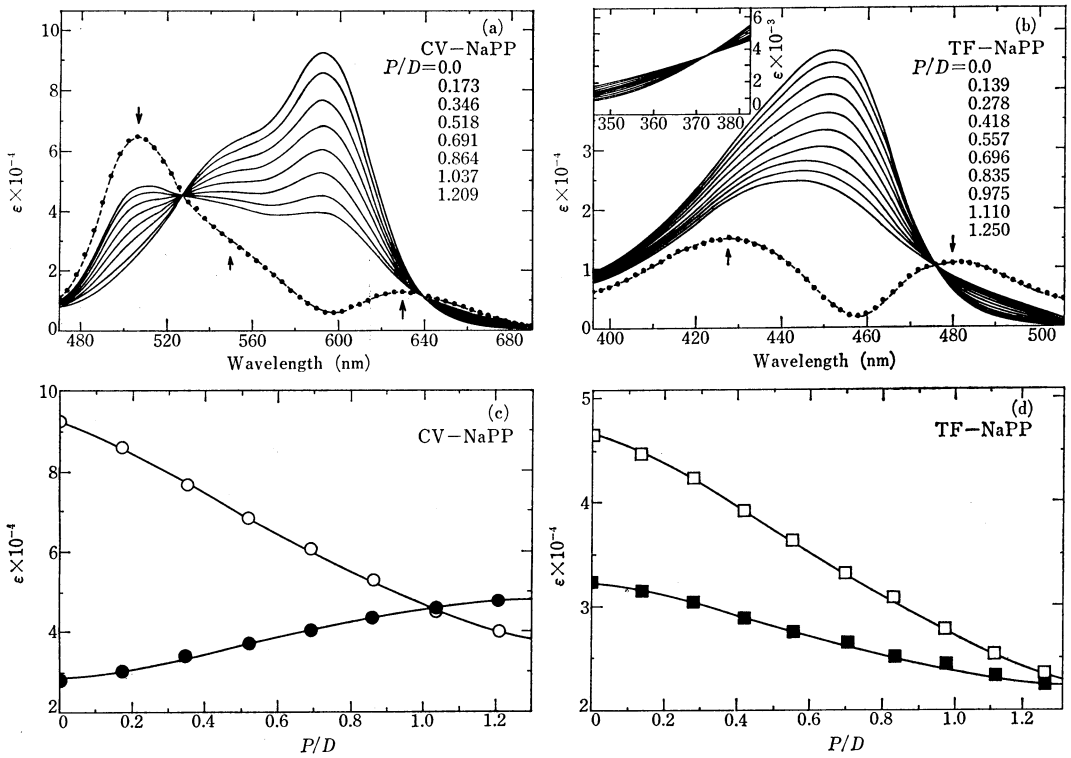

Fig. 1. Absorption spectra of CV and TF (solid curves) in the presence and absence of NaPP, the pure absorption spectra of bound dyes (closed circles) and optical titration curves.
The initial concentrations of CV and TF are 8.76 and 11.0 μM ((a) and (b)), respectively. The concentrations of NaPP are given in the respective figures in terms of P/D, the order of which corresponds to the order of the decrease in the maximum absorbances. The apparent molar absorption coefficients ε at 510 nm (●) and 592 nm (○) for CV and at 430 nm (■) and 450 nm (□) for TF are plotted against P/D in (c) and (d), respectively.

where K is the equilibrium constant, X_i is the ith absorbing or nonabsorbing component, and ν_i is the stoichiometric coefficient of X_i, whose equilibrium concentration is denoted by the brackets. The presence of nonabsorbing components in a given dye–polyanion system is subject to the equation of mass balance. Their equilibrium concentrations, therefore, can be calculated from their analytical concentrations and the **C** matrix if a set of the initial values for the elements of the **t** matrix is available. The substitution of m sets of the equilibrium concentrations in the right-hand side of Eq. 7 yields m different values for K, unless both the elements of the **t** matrix and the assumed equilibrium expression for the dye–polyanion system are correct. In order to discriminate the most probable **t** matrix and the equilibrium expression from the remainder, the coefficient of variation, S, is defined by Eq. 8 and used as a criterion:

$$S = \left(\frac{1}{m}\sum_{j=1}^{m}(K_j-\bar{K})^2\right)^{1/2}\Big/\bar{K}, \qquad (8)$$

where $\bar{K}$ denotes the mean value of K_j. The elements of the **t** matrix, and the equilibrium expression which yield the minimum S value can be determined by iterative calculations. The value of $\bar{K}$ corresponding to the minimized S value is considered as the most probable equilibrium constant. In this work, an acceptable upper limit of 0.15 was set for the minimized value of S in view of the experimental errors.[32]

Results

Application of the PCA Method to CV- and TF–NaPP Systems. The visible absorption spectra of CV and TF in the presence of NaPP are shown in Figs. 1(a) and (b) respectively. The spectra were measured at different stages of titration with the titrant NaPP solution up to the molar ratios of polymer residue-to-dye (P/D) of 1.21 and 1.25 for CV and TF respectively. The apparent molar absorption coefficients (ε) were calculated using the analytical concentrations of the dye in the solution. The spectra of CV–NaPP reveal a remarkable Meta band near 510 nm and three isosbestic points at 460, 529, and 639 nm (Fig. 1(a)), whereas TF–NaPP shows no such Meta band, but does show two isosbestic points at 371 and 476 nm (Fig. 1(b)). The apparent maximum absorption bands remain for CV, but are shifted gradually toward the shorter wavelengths for TF with an increase in the P/D.

The optical titration curves are plotted against P/D in terms of ε for CV and TF in Figs. 1(c) and (d) respectively. The titration curves were drawn at 510 and 592 nm for CV and at 430 and 450 nm for TF. It is clear from Figs. 1(c) and (d) that all these titration curves change with P/D sigmoidally but not monotonously. However, it can be expected from the existence of isosbestic points in the spectra of either

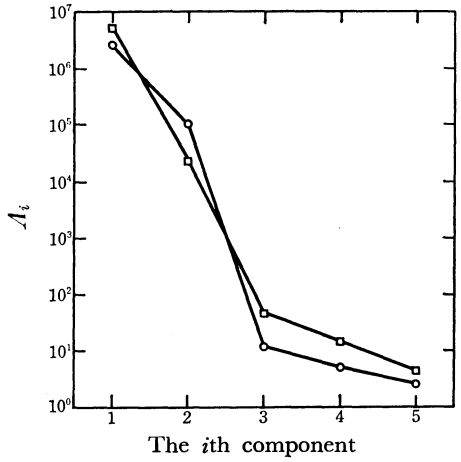

Fig. 2. Variation in eigenvalue Λ_i (i=1, 5) with the ith absorbing component. ○: CV–NaPP, □: TF–NaPP.

the CV– or TF–NaPP solution that there are two different absorbing components in the system. Such sigmoidal titration behavior was noted in the Acridine Orange–poly(α-L-glutamic acid) (PGA) system in the P/D range of 0—1 by Myhr and Foss.[15] They simply attributed the sigmoidal change to the equilibrium between three different absorbing components, *i.e.*, the free monomeric and dimeric dyes and the PGA-bound dye.

Since the advantage of the PCA method is that the likely number of the absorbing components involved in an equilibrium state can be determined by itself, it was applied to the sets of the observed spectra of dye-polyanion solutions over the entire P/D range shown in Figs. 1(a) and (b). The data matrix for CV–NaPP was composed of a set of absorbances at 56 selected wavelengths from 470 to 690 nm, at intervals of 4 nm, and a set of eight solutions differing in P/D, while the matrix for TF–NaPP was composed of a set of absorbances at 56 selected wavelengths from 396 to 512 nm, at intervals of 2 nm, and a set of ten solutions. The variations in eigenvalue Λ_i(i=1, 5) with the ith component are shown for both CV– and TF–NaPP systems in Fig. 2. It is clear that a large gap in eigenvalues exists between the second and third components for each system. This result confirms that the families of spectra in both Figs. 1(a) and (b) are composed of two, but not three, absorbing components, probably free and bound dyes. Schwarz[18] proposed a graphical method to analyze the absorption spectra of dye–polyion systems. The method, however, cannot be applied to sigmoidally changing titration curves like those of the CV– and TF–NaPP systems.

The extended PCA method is effective in analyzing the data of an unknown equilibrium system, since it assumes, successively, possible equilibrium schemes for a dye–polyanion system as *modus operandi*. Some specific equilibrium formulas based on Eq. 7 must first be considered for the equilibrium system. Three binding reactions frequently postulated for the system containing two absorbing components in the low P/D range are

$$D + P \rightleftharpoons DP,\ K = \frac{[DP]}{[D][P]}, \tag{9}$$

$$2D + PP \rightleftharpoons DPDP,\ K = \frac{[DPDP]}{[D]^2[PP]}, \tag{10}$$

and

$$D + 2P \rightleftharpoons PDP,\ K = \frac{[PDP]}{[D][P]^2}, \tag{11}$$

where D is the free, unbound dye; P is the unoccupied binding site of polyanion; DP is the complex, *i.e.*, the bound dye; PP denotes two nearest-neighboring unoccupied sites; DPDP is the dimeric unit of bound dyes, and PDP is the complex in which a dye is bound to two nonneighboring polymer sites. The unknown absorbing components are DP, DPDP, and PDP, while the nonabsorbing components are P and PP. Unless otherwise stated, the computations were carried out under the assumption that the absorption spectrum of the free dye D is known. Equations 9 and 10 showed only monotonous titration curves, whereas Eq. 11 produced sigmoidal ones. In each of these three cases, the value of S in Eq. 8 could be minimized by varying the elements of the **t** matrix iteratively. However, the **t** matrix at this minimum S yielded some negative values for the molar absorption coefficient or the equilibrium concentration of the unknown absorbing component. Hence, the three schemes (9)—(11) should be concluded to be physically unsuitable for the experimental data.

Into the above three expressions, only the binding site P was taken as a nonabsorbing component which can not be directly detected as the eigenvector by the PCA method. In addition, solvent water and the counter-ions of the dye and NaPP, *i.e.*, Cl^- and Na^+, are all present in the solution as nonabsorbing components. Water is the solvent, so its concentration should be constant in equilibrium systems.[42] Consequently, the counter-ion Cl^- was taken into the fourth equilibrium scheme for the formation of a dye-polymer complex as follows:

$$D + Cl^- + P \rightleftharpoons DClP^-,$$
$$K = \frac{[DClP^-]}{[D][Cl^-][P]} = \frac{[DClP^-]}{[D]^2[P]}, \tag{12}$$

where $DClP^-$ is the complex and where $[D]=[Cl^-]$. No sigmoidal titration curve could be simulated with Eq. 12. Some K values calculated from the **t** matrix, which minimized S, deviated greatly from the mean value $\bar{K}$; moreover, some of them became negative. Thus, the equilibrium scheme (12) is also unsuitable for the CV– and TF–NaPP systems.

As the fifth equilibrium scheme, the participation of the counter-ion Na^+ was assumed:

$$D + Na^+ + P \rightleftharpoons DNaP^+,\ K = \frac{[DNaP^+]}{[D][Na^+][P]}, \tag{13}$$

where $DNaP^+$ is the complex and an absorbing component with an absorption spectrum different from that of free dye. Since the initial concentration of Na^+ is equal to that of the binding site of NaPP, Eq. 13 is reduced to

$$K = \frac{[DNaP^+]}{[D][P]^2}, \tag{14}$$

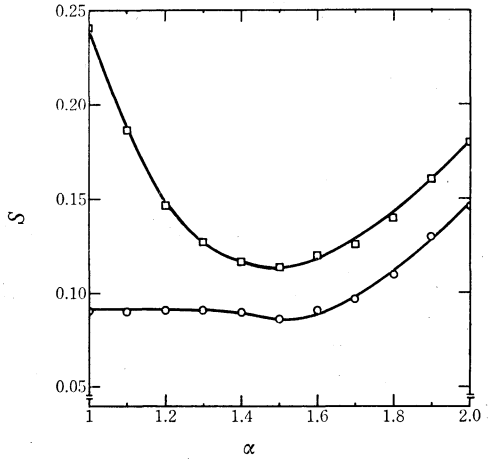

Fig. 3. Variation in the minimized S values with the empirical parameter α for the equilibrium formula (15) (see text). ○: CV–NaPP, □: TF–NaPP.

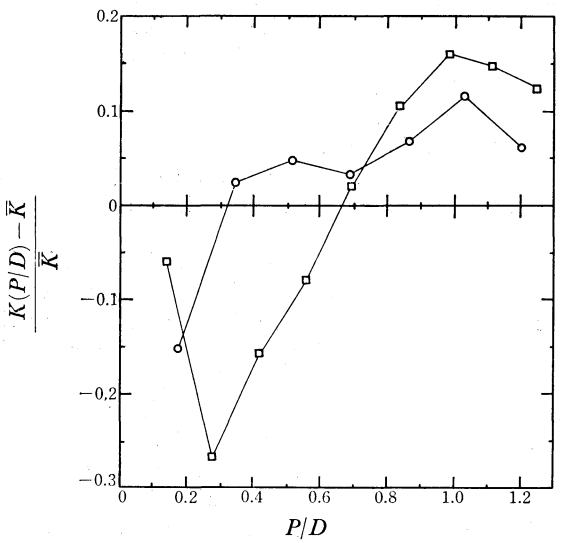

Fig. 4. Deviation of the equilibrium constant K from the mean value $\bar{K}$ at various P/D. The K values are computed with the optimum value of α in Eq. 15. ○: CV–NaPP, □: TF–NaPP.

A considerable sigmoidal change was manifested in the titration curve which was simulated with Eq. 14. Although the ε^b's of the bound dye and the values of K were always positive, the value of S was converged no less than 0.2, which exceeds the preset upper limit of 0.15.

The results of the above five equilibrium schemes led to the following conclusions. If the exponent of [D] is equal to, or larger than, that of [P], the optical titration data give rise to a monotonous curve. On the other hand, if the exponent of [P] is larger than that of [D], a sigmoidal titration curve results. Therefore, Eq. 14 is generalized by introducing an empirical parameter α into the equilibrium expression as

$$K = \frac{[DP^*]}{[D][P]^\alpha}, \qquad (15)$$

where DP* is the bound dye which differs from the free dye as regards the absorption spectrum. Both

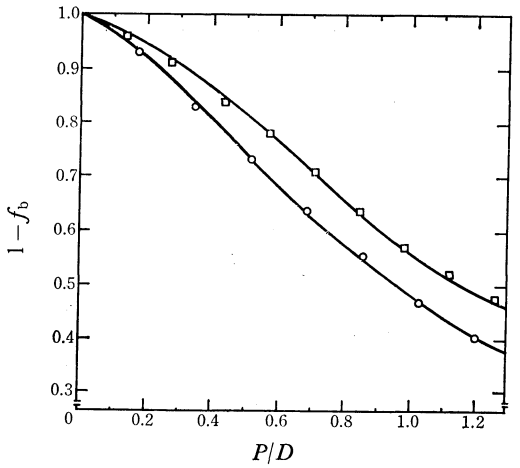

Fig. 5. Variation in the fraction of free dye $(1-f_b)$ with P/D for CV– and TF–NaPP. The fractions calculated at each P/D from Eq. 6 are represented by (—○—) and (—□—) for CV and TF, respectively. The fractions calculated from Eq. 15 with the values of α and the corresponding K given in Table 3 are drawn with solid curves.

monotonous and sigmoidal titration curves of various types can be produced from Eq. 15 by varying the parameter α.

Figure 3 shows the variations in the S values minimized by the **t** matrix with the empirical parameter α in Eq. 15 for both CV– and TF–NaPP systems. With an α value of 1.5, the values of S for the CV– and TF–NaPP systems reach the minimum points of 0.08 and 0.113 respectively. Both points are below the limit of 0.15. The variations in K with P/D at these points of S are shown in Fig. 4 for CV– and TF–NaPP. The scattering of each K from the mean value is only moderate, showing no systematic trend. These results suggest that equilibrium scheme (15) is acceptable for the binding reaction between NaPP and CV or TF if α is taken as 1.5.

The **t** matrix elements which minimized the S value are used for the calculation of the pure spectrum of the bound dye in terms of the molar absorption coefficient at the wavelength λ, ε^b_λ, determined in accordance with Eq. 5. The pure spectra of bound CV and TF are shown by closed circles in Figs. 1(a) and (b) respectively. The pure spectrum of bound CV reveals two peaks and a shoulder, while that of bound TF reveals two peaks (indicated by arrows). Although the Meta band of TF is not discernible at all in the observed spectra, the pure spectrum of bound TF demonstrates that a band does exist in the wavelength region shorter than the dominant peak of free TF. The characteristics of these spectra of bound dyes will be discussed later. Lastly, it should be noted that similar calculations were carried out with an assumption that the spectrum of the free dye D is unknown. The simulated spectrum of the free dye under this condition became identical to the observed one with $\alpha=1.5$ in Eq. 15.

The fraction of the bound dye, f_b, defined as C_b/C, could also be calculated at each P/D from the same

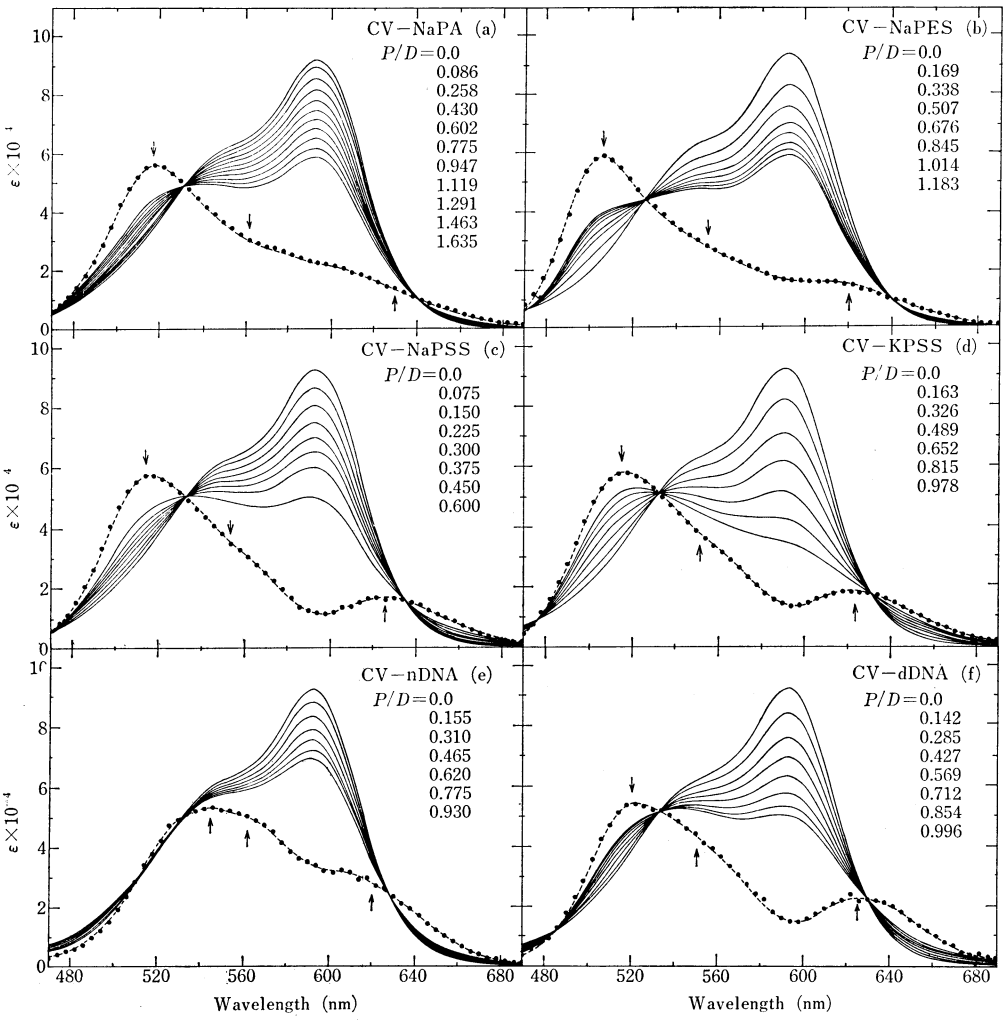

Fig. 6. Absorption spectra of CV in the presence and absence of polyanions (solid curves) and the pure absorption spectra of bound CV (closed circles).
Polyanions are; (a) NaPA, (b) NaPES, (c) NaPSS, (d) KPSS, (e) nDNA, and (f) dDNA. Neither polyanion nor dye solution contains neutral or buffer salts except for the DNA-dye solutions in which 1 mM NaCl is always present. The concentrations of CV are: (a) 8.33 μM, (b) 8.51 μM, (c) 8.67 μM, (d) 9.08 μM, (e) 9.05 μM, and (f) 11.9 μM. The concentrations of polyanions are listed in each figure in terms of P/D, the order of which corresponds to the order of the decrease in maximum absorbances. The isosbestic points are at (a) 476, 533, and 642 nm, (b) 460, 526, and 641 nm, (c) 473, 532, and 631 nm, (d) 473, 532, and 631 nm, (e) 628 nm, and (f) 486, 533, and 631 nm.

elements of the **t** matrix in accordance with Eq. 6, where C_b and C are the concentrations of the bound dye and the sum of the bound and free dyes respectively. The C_b at a given P/D is the mean of the C_b^λ values calculated from the observed spectrum at selected wavelengths, where C_b^λ is equal to $C(\varepsilon_\lambda - \varepsilon_\lambda^f)/(\varepsilon_\lambda^b - \varepsilon_\lambda^f)$. Therefore, the points in Fig. 5 represent the mean values of the normalized observed optical titration curves at selected wavelengths for CV- and TF-NaPP (circles and squares). These results are compared with the fractions of bound dye which were calculated from Eq. 15 with the values of α (=1.5) and K in Table 3; they are plotted with solid lines in Fig. 5. The agreement between them is excellent for both CV- and TF-NaPP. It should be noted that the sigmoidal decrease in the fraction of the unbound dye $(1-f_b)$ is quite clear.

Application of the PCA Method to Some CV-Polyelectrolyte Systems. Six polyelectrolytes, NaPA, NaPES, NaPSS, KPSS, nDNA, and dDNA, are chosen. The backbone structure of NaPA, NaPES, and NaPSS is identical, but their functional groups differ from one another. The difference between NaPSS and KPSS is only for the counter-ion, while nDNA and dDNA as biopolymers are different only in conformation. The absorption spectra of CV titrated with each polyanion are shown in Figs. 6(a)—(f). In all cases, the apparent ε at 592 nm decreases with the increase in P/D. The appearance of the Meta band in the observed spectra depends on the kind of polyanion; that is, a typical Meta band of CV appears near 510 nm in the presence of KPSS, whereas the Meta band appears only as a shoulder in the presence of NaPA, NaPES, and NaPSS. The presence of the Meta band is not manifested in the nDNA and dDNA. Two isosbestic points are clearly observed for each of the systems, suggesting

that two or more absorbing components are present. The eigenvalues of the second moment matrix were calculated from each set of spectra in Figs. 6(a)—(f). The ratios of the eigenvalues of the second, third, and fourth components to the eigenvalue of the first component are listed in Table 1. The ratios (expressed in terms of the logarithm) clearly indicate that a large gap exists between the second and third eigenvalues in each system, while the difference between the third and fourth eigenvalues is very small. These data verify that, in each CV–polyanion system, two absorbing components are involved in the binding reaction.

The pure spectra of bound CV are shown by closed circles in Figs. 6(a)—(f). For all the CV–polyanion systems, they exhibit two bands: a peak and a shoulder in the shorter-wavelength region and a band in the wavelength region longer than the peak position of free CV. These absorption bands will hereafter be abbreviated as follows: the Meta S_1 and Meta S_2 bands for the shorter-wavelength ones and the Meta L band for the longer-wavelength one (the numbering is from the one closest to the peak position of the free dye). The locations and ε^b's of the three Meta bands all depend on the polyanions, as is shown in Fig. 6 and Table 2. Especially, the Meta S_1 and S_2 bands of nDNA and dDNA seem to reflect their different conformations (the double helix *vs.* single-stranded coil).

TABLE 1. THE SECOND, THIRD, AND FOURTH EIGENVALUES NORMALIZED TO THE FIRST EIGENVALUE FOR CV- AND TF-POLYANION SYSTEMS

Dye	Polyanion	$\log(\Lambda_2/\Lambda_1)$	$\log(\Lambda_3/\Lambda_1)$	$\log(\Lambda_4/\Lambda_1)$
CV	NaPP	−1.39	−5.36	−5.72
	NaPA	−2.29	−5.46	−5.71
	NaPES	−2.14	−5.00	−5.60
	NaPSS	−2.09	−5.72	−5.91
	KPSS	−1.61	−4.90	−5.79
	nDNA	−2.90	−5.16	−5.68
	dDNA	−2.60	−4.97	−5.21
TF	NaPP	−2.34	−5.02	−5.55
	NaPA	−3.25	−5.80	−6.16
	NaPES	−2.68	−5.08	−5.74
	NaPSS	−2.17	−5.37	−5.69
	KPSS	−2.26	−5.59	−5.70
	nDNA	−2.89	−5.08	−6.02
	dDNA	−2.47	−4.63	−5.03

The optical titration curves of CV at 592 and 510 nm with six polyanions were found to be divided into two classes. Sigmoidal titration curves were observed for NaPA and KPSS just for NaPP (Fig. 5) and monotonous curves for NaPSS, NaPES, nDNA, and dDNA. The fractions of the bound dye, f_b, were calculated from Eq. 6; they are shown in Figs. 7(a)—(f). With the values of α and K which gave rise to the smallest S (the values are listed in Table 3 for each system), the observed titration curve can be reproduced quite excellently, as is indicated by the solid lines. It should be noted that the sigmoidal titration curve was observed whenever the value of α is greater than one, while a monotonous titration curve resulted when the value of α is equal to, or less than, one.

Application of the PCA Method to Some TF–Polyelectrolyte Systems. The same six polyanions are also

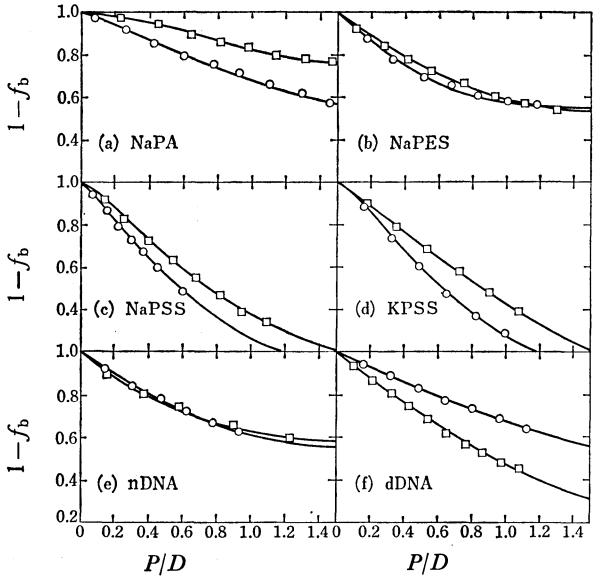

Fig. 7. Variation in the fraction of free dye ($1-f_b$) with P/D for six dye-polyanion systems. ○: CV-polyanions, □: TF-polyanions. For other details, see the caption of Fig. 5.

TABLE 2. THE MOLAR ABSORPTION COEFFICIENTS, ε^b, AND LOCATIONS OF METACHROMASY BANDS OF CV AND TF BOUND TO VARIOUS POLYANIONS

	Dye	CV ($\lambda_{max}=592$ nm; $\varepsilon=9.20\times10^4$)						TF ($\lambda_{max}=452$ nm; $\varepsilon=4.67\times10^4$)			
	Band	Meta S_2		Meta S_1[a)]		Meta L		Meta S		Meta L	
		λ(nm)	$\varepsilon^b\times10^{-4}$	λ(nm)	$\varepsilon^b\times10^{-4}$	λ(nm)	$\varepsilon^b\times10^{-4}$	λ(nm)	$\varepsilon^b\times10^{-4}$	λ(nm)	$\varepsilon^b\times10^{-4}$
Polyanion	NaPP	506	6.48	550	2.97	630	1.26	428	1.53	480	1.08
	NaPA	518	5.41	550	3.54	630	1.53	430	1.35	475	1.17
	NaPES	506	5.78	555	2.72	620	1·52	430	1.85	476	0.96
	NaPSS	514	5.73	550	3.79	625	1.66	438	1.78	476	1.53
	KPSS	516	5.77	550	3.86	625	1.80	438	1.74	476	1.53
	nDNA	545	5.28	560	5.03	620	2.83	444	2.12	466	2.69
	dDNA	520	5.38	550	4.39	625	2.26	437	2.28	472	1.11

a) The position of this band is only approximate.

Table 3. Empirical parameters, α, and equilibrium constants, K and K', at 25 °C for CV- and TF-polyanion systems

	Dye	CV			TF		
		α	K [a]	K' [b]	α	K [a]	K' [b]
Polyanion	NaPP	1.5	$(1.0\pm0.1)\times10^{8}$	2.1×10^{5}	1.5	$(5.1\pm0.3)\times10^{7}$	1.3×10^{5}
	NaPA	1.2	$(8.8\pm0.9)\times10^{5}$	0.79×10^{5}	1.2	$(2.4\pm0.2)\times10^{5}$	0.24×10^{5}
	NaPES	0.6	$(1.1\pm0.1)\times10^{3}$	1.5×10^{5}	0.9	$(4.9\pm0.6)\times10^{4}$	1.7×10^{5}
	NaPSS	0.9	$(3.7\pm0.3)\times10^{5}$	13×10^{5}	1.5	$(2.6\pm0.1)\times10^{8}$	4.9×10^{5}
	KPSS	1.5	$(8.3\pm0.6)\times10^{8}$	12×10^{5}	1.3	$(1.6\pm0.2)\times10^{7}$	3.7×10^{5}
	nDNA	1.0	$(1.30\pm0.05)\times10^{5}$	1.3×10^{5}	1.0	$(7.4\pm0.6)\times10^{5}$	7.4×10^{5}
	dDNA	1.0	$(1.30\pm0.05)\times10^{5}$	1.3×10^{5}	1.0	$(1.8\pm0.3)\times10^{5}$	1.8×10^{5}

a) The dimension is given by $[\mathrm{l/mol}]^{\alpha}$. b) $K'=K\cdot[\mathrm{P}]^{\alpha-1}$ at $P/D=1$.

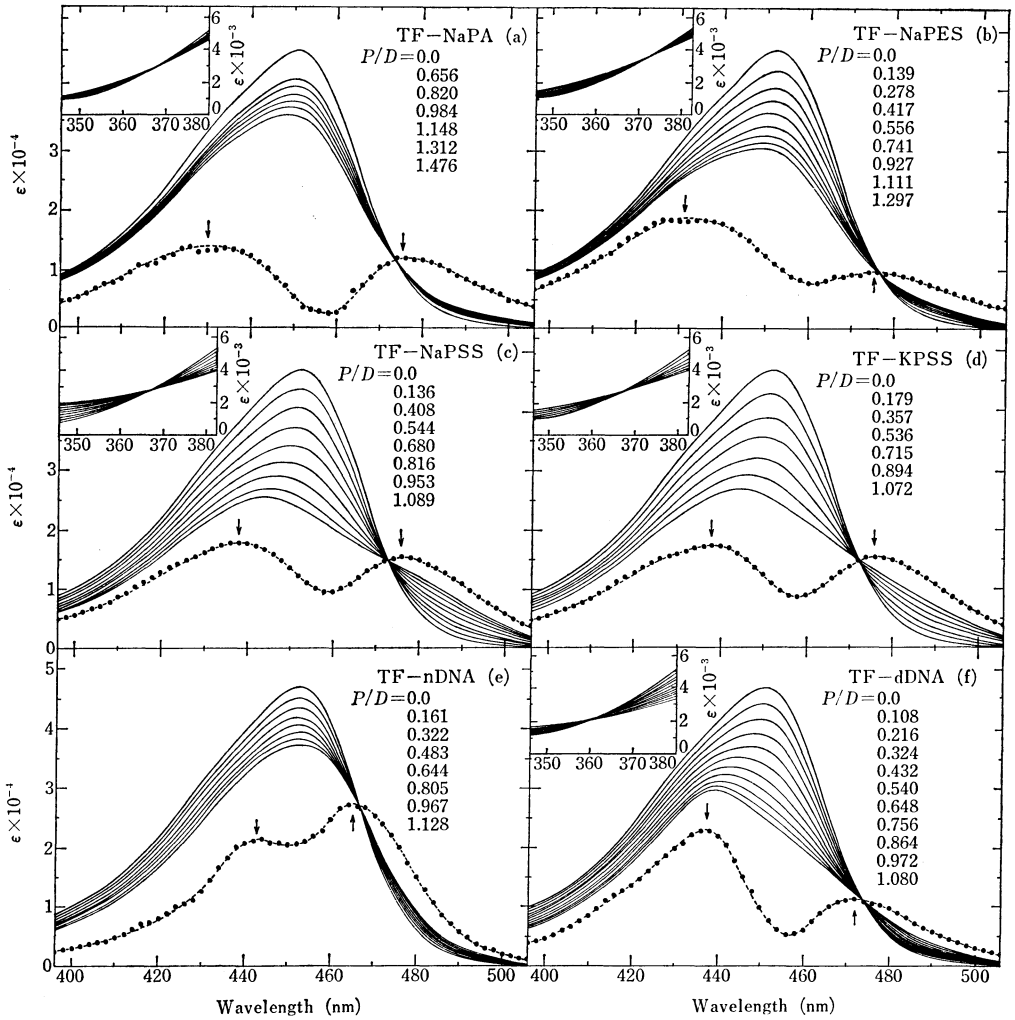

Fig. 8. Absorption spectra of TF in the presence and absence of polyanions (solid curves) and pure absorption spectra of bound TF (closed circles).
Polyanions are; (a) NaPA, (b) NaPES, (c) NaPSS, (d) KPSS, (e) nDNA, and (f) dDNA. Neither polyanion nor dye solution contains neutral or buffer salts except for the DNA–dye solutions in which 1 mM NaCl is always present. The concentrations of TF are: (a) 11.0 μM, (b) 7.77 μM, (c) 9.56 μM, (d) 8.28 μM, (e) 8.69 μM, and (f) 11.0 μM. The concentrations of polyanions are listed in each figure in terms of P/D, the order of which corresponds to the order of the decrease in maximum absorbances. The isosbestic points are at (a) 369 and 473.5 nm, (b) 372 and 476 nm, (c) 368 and 472 nm, (d) 368 and 472 nm, (e) 466 nm, and (f) 359 and 474.5 nm.

used for the titration of TF; the results are shown in Figs. 8(a)—(f). The spectra of all the TF–polyanion systems differ from those of the corresponding CV–polyanion systems in showing hypo- and hypsochromic effects without any Meta bands in the P/D range examined. The spectra of TF in the presence of polyanions show, without exception, an isosbestic point in the wavelength region longer than the peak position of the free TF. Another isosbestic point is also noted in the shorter-wavelength region (*cf.* the insert in each figure) except for the case of nDNA. Judged from the eigenvalues listed in Table 1, only two absorbing components are again sufficient to describe the spectral behavior in each TF–polyanion system. The pure spectra of bound TF are shown by closed circles in Figs. 8(a)—(f). Although none of the observed spectra manifests the presence of the Meta band, the bound spectra clearly show two such bands—the Meta S and Meta L bands — in all cases. The spectral profiles of the bound TF differ from those of the bound CV as regards the number of bands. The locations and ε^b's of those two Meta bands depend on the kinds of polyanions. They are listed in Table 2.

The empirical parameter α and the equilibrium constant K in Eq. 15 at the minimized S, which result from the application of the PCA method to the TF–polyanion spectra, are listed in Table 3 for all the systems. The values of α are, again, greater than one for those systems which yield the sigmoidal titration curves, whereas the values of α are equal to, or less than, one for those systems which produce the monotonous curves. As is shown in Figs. 7(a)—(f), the optical titration curves are sigmoidal for NaPA, NaPSS, and KPSS just for NaPP (*cf.* Fig. 5), while they are monotonous for NaPES, nDNA, and dDNA. The value of α obtained for the TF–polyanion system, however, is not necessarily identical with the value of α for the corresponding CV–polyanion system. This suggests that the value of α reflects the complexity and diversity of the binding reaction between a dye and a polyanion, the importance of the combination thereof, and the specificity of the chemical structure of the dye. It should also be noted in Fig. 7 that the fraction of the free, unbound dye decreases with the increase in the value of P/D, while no simple relation exists between TF and CV as regards their binding ability toward polyanions.

Discussion

The Method of Extended Principal Component Analysis. As has been described in a previous paper,[32] the PCA method has been proven to be exceedingly useful for an equilibrium system like dilute dye solutions composed of two or three absorbing components. In the equilibrium system of small molecules, the equilibrium schemes are relatively simple and the neglect of such a thermodynamic variable as activity coefficient may not affect the result too seriously. On the other hand, the binding of a dye to the polymer site is probably influenced by a large number of complicated factors in dye–polymer systems. In order to estimate the equilibrium scheme and the binding constant for these systems, and in order to evaluate the bound-dye spectrum, the equilibrium concentrations of the colored components have usually been determined by means of the absorption spectra and equilibrium dialysis combined.[12,16,20,27,31] Such a combined method, however, is difficult to apply to systems in which either a relatively small polymer cannot be retained by a semipermeable membrane, a dye is easily adsorbed on it, or the ionic strength imposes severe limitations as a result of the Donnan effect.

On the other hand, only the initial concentrations of the chemical species participating in a binding reaction and a set of the absorption spectra of solutions are needed in the PCA method; therefore, using it, a number of plausible equilibrium schemes can be tested successively. In order to determine the most probable absorption spectra of colored components and the equilibrium constant for the binding reaction, the only requirements are that the coefficient of variation S should reach a preset minimum value and that none of the spectra and equilibrium concentrations of the components should have a negative value. The latter condition is imposed by the physical restrictions and is quite useful for selecting appropriate parameters.[32] Thus, the only problem is concerned with the availability of adequate equilibrium expressions which describe the complicated binding processes between the dye and the polymer. In this work, an empirical parameter α was introduced into a relatively simple expression (Eq. 15) to circumvent the complexity. Since the PCA method could be applied to multicomponent dye systems,[32] its use may also be extended in the future to the dye–polyelectrolyte systems over the whole P/D range where more than two absorbing components coexist.

Absorption Spectra of Bound CV and TF. The term "metachromasy" has been used for the phenomenon of the hypo- and hypsochromic changes of the spectrum of a dye, often with a new band on the short-wavelength side which has been called the "metachromasy band." However, this concept of metachromasy is an oversimplification, as has been pointed out by a number of reports which more or less emphasize the simultaneous bathochromic effect of various polyelectrolytes on the spectrum of the dye.[1–3,43–45] The present work has proven that both bound CV and TF exhibit absorption spectra in which the new bands are clearly unraveled on the short- and long-wavelength sides of the peak of the corresponding free dyes (Figs. 1, 6, and 8). Fredericq and Houssier[16] have observed a similar result in the Acridine Orange–DNA system. The term "metachromasy band" may now be enlarged to include the long- and short-wavelength bands of a bound dye, both of which are abbreviated as "Meta bands."

The Meta S band for TF and the Meta L band for CV and TF are close to the peak of the free dyes and are simply hidden in the observed spectra, although their presence has been predicted from linear and circular dichroic studies.[44–47] The locations and ε^b's of the Meta bands for a given dye depend on the poly-

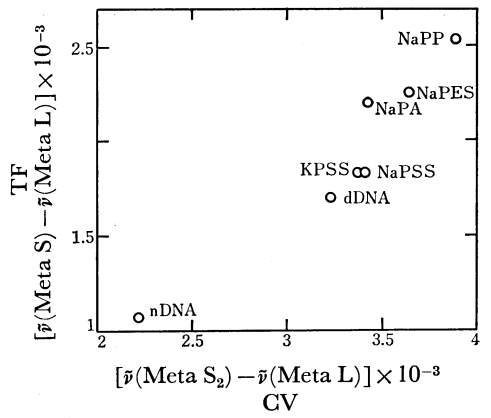

Fig. 9. Correlation between the energy separation between the Meta S_2 and L bands of CV and the separation between the Meta S and L bands of TF bound to seven polyanions. Scales are expressed in terms of wavenumbers $\tilde{\nu}$.

anions (Table 2). The Meta bands of CV and TF bound to NaPA, NaPES, and NaPSS differ from one another depending on their functional groups, in spite of the fact that their backbone structure is identical. On the other hand, the Meta bands of nDNA and dDNA differ considerably in shape and position, although their backbone and functional groups are also identical. The Meta bands of either TF or CV are almost identical for NaPSS and KPSS. These results lead to the conclusion that the Meta bands sharply reflect the conformation of dye–polyanion complexes besides the functional group of the polyanions and that the kind of counter-ion scarcely affects the location and ε^b of the Meta bands.

A considerable positive correlation exists between the energy separation between the Meta S_2 and L bands of CV and the separation between the Meta S and L bands of TF, as is shown in Fig. 9; this indicates that the peak position of Meta bands depend mainly on the overall nature of the polyanions. The energy separation between the Meta S and L bands for a given dye may result from the different mean distance between the binding sites of a polyanion. The mean distance may, in turn, depend on the flexibility of the backbone in addition to the structure of the sidechain of the polyanion. The spectral aspects of the Meta band of bound dyes have now been clarified in sufficient detail. For a quantitative discussion of metachromasy, however, information is necessary on the electronic states and transition moments of dyes in the absence and presence of polyanions. The LCAO calculations may provide such information.

Empirical Parameter α and Equilibrium Constant. The absorption spectra of solutions containing both a dye and a polyanion vary in a complicated manner when a wide range of P/D is covered.[1–3] For example, the isosbestic points appear at different wavelengths depending on the P/D range, as has already been noted for CV– and TF–NaPP systems.[2,3] This strongly suggests that two or more of the absorbing components, *i.e.*, the bound dye species exclusive of the free dye, are present over the whole P/D range. In this work, the spectral changes in each dye–polyanion system are limited only in the low P/D range of 0—1, where a single set of isosbestic points is observed. In this P/D range, only a free dye and one kind of bound dye are present, as is confirmed by the eigenvalues of the second moment matrix (*cf.* Table 1). The empirical parameter α is indeed useful in simulating the optical titration curves and in classifying the dye–polyanion systems (Figs. 1 and 7). However, the values of the equilibrium constant K as such cannot be compared in order to characterize the different dye–polyanion systems, because the dimension of K ($=[\text{l/mol}]^{\alpha}$) now depends on α and is not identical in all the systems. The constant K defined in Eq. 15 may be related to the frequently granted equilibrium constant K' for the binding scheme (9) in such a way that $K'=[\text{DP}]/[\text{D}]\cdot[\text{P}]=K\cdot[\text{P}]^{\alpha-1}$. The values of K' calculated at $P/D=1$ using the K values listed in Table 3 are also given in the same table. Interestingly, these K' values compare favorably with the binding constants previously reported for various dye–polymer systems.[8,12,16,18,31]

The values of α for NaPA, NaPES, NaPSS, and KPSS differ from one another in ways reflecting the difference in the functional group or counter-ion of the polyanions (Table 3). Moreover, the α values also depend on the kind of dye to some extent. The difference in α-value between NaPSS and KPSS in the presence of either CV or TF suggests that the counter-ion plays some important role in the binding process of the dye to the polyanion, but does not affect the bound spectra. On the other hand, the values of α are unity for the dye–DNA systems and independent of the kinds of dyes and conformations of DNA, for which the distance between the charged sites of DNA appears to be responsible. Hence, the parameter α may be an indicator which reflects the local situation of the binding site of the polyanion, including the conformation, functional group, the counter-ion, and the structure and binding mode of the dye. Although the value of α is at present regarded as a constant in a low P/D range, it may be a function of P/D and could also represent the dependence of the activity coefficient of the polyelectrolyte on the residue concentration. Once the physical significance of the parameter α is clarified, it should be of great help for the better understanding of the metachromatic behavior of dye–polyelectrolytes. However, the parameter seems to contain many factors, such as temperature, counter-ion, and added salts. Thus, the clarification of the nature of α still awaits further quantitative studies.

Conclusions

The extended PCA method has now been demonstrated to be applicable to relatively complicated equilibrium systems between dyes and polyanions. By the use of this method, the quantitative studies of metachromasy are greatly facilitated as regards the number of dye species involved in dye–polyanion systems in equilibrium, the equilibrium constants, and the pure absorption spectra of the bound dye species. For each dye–polyanion system presently studied in

the low P/D range between zero and near one, only a single bound dye species is present besides a free, unbound dye. The pure spectra of bound CV and TF both show two remarkable metachromasy bands on the short- and long-wavelength sides of the absorption peak of free, unbound dyes. The spectral features of these bands are related to the functional group and the conformation of the polyanions. The equilibrium scheme between the bound and unbound absorbing components is not so simple as is often assumed, but requires an empirical parameter α to reproduce satisfactorily both the sigmoidal and monotonous optical titration curves of CV and TF. This parameter is probably an indicator of the local situation of the dye-bound polymer sites.

References

1) K. Yamaoka, T. Suenaga, A. Fujita, and M. Miura, *J. Sci. Hiroshima Univ., Ser. A*-II, **34**, 1 (1970).
2) K. Yamaoka, M. Takatsuki, Y. Yaguchi, and M. Miura, *Bull. Chem. Soc. Jpn.*, **47**, 611 (1974).
3) K. Yamaoka, M. Takatsuki, and M. Miura, *Bull. Chem. Soc. Jpn.*, **48**, 2739 (1975).
4) G. Weill and M. Calvin, *Biopolymers*, **1**, 401 (1963).
5) R. E. Kay, E. R. Walwick, and C. K. Gifford, *J. Phys. Chem.*, **68**, 1896 (1964).
6) R. C. Bean, W. C. Shepherd, R. E. Kay, and E. R. Walwick, *J. Phys. Chem.*, **69**, 4368 (1965).
7) T. Soda, and K. Yoshioka, *Nippon Kagaku Zasshi*, **87**, 22 (1966).
8) R. K. Tubbs, W. E. Ditmars, Jr., and Q. V. Winkle, *J. Mol. Biol.*, **9**, 545 (1964).
9) H. Ito and Y. J. I'Haya, *Int. J. Quantum Chem.*, **2**, 5 (1968).
10) V. Kleinwächter and J. Koudelka, *Biophysik*, **5**, 119 (1968).
11) D. G. Dalgleish, H. Fujita, and A. R. Peacocke, *Biopolymers*, **8**, 633 (1969).
12) D. G. Dalgleish, M. C. Feil, and A. R. Peacocke, *Biopolymers*, **11**, 2415 (1972).
13) M. K. Pal and M. Chauduri, *Makromol. Chem.*, **133**, 151 (1970).
14) M. K. Pal and M. Biswas, *Makromol. Chem.*, **151**, 121 (1972).
15) B. C. Myhr and J. G. Foss, *Biopolymers*, **10**, 425 (1971).
16) E. Fredericq and C. Houssier, *Biopolymers*, **11**, 2281 (1972).
17) G. Löber, H. Schütz, and V. Kleinwächter, *Biopolymers*, **11**, 2439 (1972).
18) G. Schwarz, S. Klose, and W. Balthasar, *Eur. J. Biochem.*, **12**, 454 (1970).
19) W. H. J. Stork, P. L. de Haseth, W. B. Schippers, C. M. Körmeling, and M. Mandel, *J. Phys. Chem.*, **77**, 1772 (1973).
20) W. H. J. Stork, J. A. M. Van Boxsel, A. F. P. M. de Goeij, P. L. de Haseth, and M. Mandel, *Biophys. Chem.*, **2**, 127 (1974).
21) S. C. Guhaniyogi and B. M. Mandel, *Makromol. Chem.*, **175**, 823 (1974).
22) V. Vitagliano, L. Costantino, and A. Zagari, *J. Phys. Chem.*, **77**, 204 (1973).
23) V. Vitagliano, L. Costantino, and R. Sartorio, *J. Phys. Chem.*, **80**, 959 (1976).
24) G. Löber, J. Koudelka, and E. Smekal, *Biophys. Chem.*, **2**, 158 (1974).
25) M. Tsuda, *Bull. Chem. Soc. Jpn.*, **48**, 1709 (1975).
26) S. Ichimura, *Biopolymers*, **14**, 1033 (1975).
27) J. S. Tan and R. L. Schneider, *J. Phys. Chem.*, **79**, 1380 (1975).
28) M. K. Salter, W. B. Rippon, and E. W. Abrahamson, *Biopolymers*, **15**, 1213 (1976).
29) M. Shirai, T. Nagatsuka, and M. Tanaka, *Chem. Lett.*, **1976**, 291.
30) M. Shirai, T. Nagatsuka, and M. Tanaka, *Makromol. Chem.*, **178**, 37 (1977).
31) K. Yamaoka and M. Masujima, *Biopolymers*, in press.
32) M. Takatsuki, and K. Yamaoka, *J. Sci. Hiroshima Univ. Ser. A*, **40**, 387 (1976).
33) W. H. J. Stork, G. J. M. Lippits, and M. Mandel, *J. Phys. Chem.*, **76**, 1772 (1972).
34) M. E. Lamm and D. M. Neville, Jr., *J. Phys. Chem.* **69**, 3872 (1965).
35) K. K. Rohatgi and G. S. Singhal, *J. Phys. Chem.*, **70**, 1695 (1966).
36) N. E. Sharpless, C. L. Greenblatt, and W. H. Jennings, *Trans. N. Y. Acad. Sci.*, **35**, 187 (1973).
37) W. H. Lawton and E. A. Sylvestre, *Technometrics*, **13**, 617 (1971).
38) N. Ohta, *Anal. Chem.*, **45**, 553 (1973).
39) T. W. Anderson, *Ann. Math. Statist.*, **34**, 122 (1963).
40) D. F. Bradley, I. Tinoco, Jr., and R. W. Woody, *Biopolymers*, **1**, 239 (1963).
41) S. Inoue, K. Yamaoka, and M. Miura, *J. Sci. Hiroshima Univ., Ser. A*, **39**, 27 (1975).
42) W. J. Moore, "Physical Chemistry," 3rd ed, Prentice-Hall, Englewood Cliff, N. J. (1962), Chap. 9.
43) J. A. Bergeron and M. Singer, *J. Biophys. Biochem. Cytol.*, **4**, 433 (1958).
44) K. Yamaoka and R. A. Resnik, *J. Phys. Chem.*, **70**, 4051 (1966).
45) K. Yamaoka and R. Resnik, *Nature*, **213**, 1031 (1967).
46) K. Yamaoka, *Chem. Lett.*, **1973**, 305.
47) K. Yamaoka and H. Hashimoto, *Chem. Lett.*, **1976**, 465.